CELL REGULATION, Vol. 2, 827–840, October 1991

Epidermal growth factor-stimulated calcium ion transients in individual A431 cells: initiation kinetics and ligand concentration dependence

Tamara E. Cheyette* and David J. Gross
Department of Biochemistry
and Program in Molecular and Cellular Biology
University of Massachusetts
Amherst, Massachusetts 01003

The A431 epidermoid carcinoma cell line responds to epidermal growth factor (EGF) stimulation with a number of rapid changes, including alterations in free cytosolic calcium ion concentration ($[Ca^{2+}]_i$). At the single cell level, these changes in $[Ca^{2+}]_i$ are known to proceed after a clear lag phase subsequent to EGF stimulus (Gonzalez *et al.*, 1988). The present study explores the dependence on EGF concentration of this early $[Ca^{2+}]_i$ signal. High levels of EGF (9.0–4.3 nM) produce a $[Ca^{2+}]_i$ spike followed by an elevation of $[Ca^{2+}]_i$ above basal levels. The time of initiation of the spike varies from 5 to 9 s at the high dose and from 8 to 32 s at the low dose in cells that respond. A lower level of EGF (1.5 nM) produces $[Ca^{2+}]_i$ oscillations with no prolonged elevation over basal $[Ca^{2+}]_i$. The initiation of response at this [EGF] ranges from 20 to 410 s. Intermediate stimulus levels generate $[Ca^{2+}]_i$ responses that are kinetic admixtures of these limiting responses. A simple model based on the enzymatically amplified signal cascade from ligand binding through Ca^{2+} release or influx is examined. The model predicts a prolonged lag phase followed by a rapid increase in the $[Ca^{2+}]_i$ signal that compares favorably with the data reported here.

Introduction

One of the earliest physiological changes that occurs in response to epidermal growth factor (EGF)[1] stimulation in several cell lines, including human epidermoid carcinoma A431 cells, is a rapid but transient rise in free cytosolic calcium ion activity ($[Ca^{2+}]_i$) (Sawyer and Cohen, 1981; Moolenaar *et al.*, 1986; Chen *et al.*, 1987; Hepler *et al.*, 1987; Pandiella *et al.*, 1987; Gonzalez *et al.*, 1988). The EGF-stimulated rise in $[Ca^{2+}]_i$ in A431 cells has previously been described as both time and dose dependent with a response to stimulation at concentrations as low as 1.7 nM (Moolenaar *et al.*, 1986; Hepler *et al.*, 1987; Gonzalez *et al.*, 1988). Such a rise has also been shown to be heterogeneous between individual cells, both in the extent of change in $[Ca^{2+}]_i$ and in the lag time before such a response occurs in A431 cells (Gonzalez *et al.*, 1988) and in transfected B82 or Chinese hamster ovary cells (Chen *et al.*, 1987). The latter study showed that tyrosine kinase activity of the EGF receptor (EGF-R) was necessary for a rise in $[Ca^{2+}]_i$ in response to EGF stimulation, as did a study by Moolenaar *et al.* (1988). The lag time for large doses of EGF is under 10 s (Moolenaar *et al.*, 1986; Gonzalez *et al.*, 1988; Mozhayeva *et al.*, 1989), whereas the lag time for smaller doses can be much longer. Additionally, the lag between stimulus and response varies considerably from cell to cell.

Present evidence indicates that calcium may be mobilized from both the extracellular medium and intracellular Ca^{2+} stores. Two groups, Moolenaar *et al.* (1986) and Gonzalez *et al.* (1988), reported that they were unable to stimulate a $[Ca^{2+}]_i$ response in A431 cells after a challenge with EGF applied in calcium-free medium, whereas Pandiella *et al.* (1987) and Hepler *et al.* (1987) reported that they were able to obtain a response to EGF in calcium-free medium. Hepler *et al.* (1987) and Gonzalez *et al.* (1988) suggested that these differences may arise from different clonal populations of A431 cells, each with its own specific response to a challenge

* Present address: Department of Molecular Physiology and Biophysics, Vanderbilt University, Nashville, TN 37232.

[1] Abbreviations used: $[Ca^{2+}]_i$, free cytosolic calcium ion concentration; CCD, charge coupled device; DAG, diacylglycerol; DMEM, Dulbecco's modified Eagle's medium; DMSO, dimethyl sulfoxide; EGF, epidermal growth factor; EGF-R, EGF receptor; EGTA, ethylene glycol-bis(β-aminoethyl ether)-*N,N,N′,N′*-tetraacetic acid; fura-2/AM, acetoxymethyl ester of fura-2; HEPES, *N*-2-hydroxyethylpiperazine-*N′*-2-ethanesulfonic acid; HBS, HEPES buffered saline; IP_3, inositol 1,4,5-trisphosphate; PIP_2, phosphatidylinositol bisphosphate; PKC, protein kinase C; PLC, phospholipase C-γ.

by EGF. Hepler *et al.* (1987) and Pandiella *et al.* (1987) also showed that $[Ca^{2+}]_i$ transients in calcium-free medium had a longer lag period, had a lower amplitude, and had a shorter duration than those in normal medium. These data suggested that calcium ion mobilization from both internal and external sources plays a role in the EGF response in A431 cells because the response is attenuated in the absence of external calcium ion. Gonzalez *et al.* (1988) agreed with this explanation and proposed that, for those cells that do not respond in the absence of calcium, the external calcium itself is important in triggering intracellular calcium mobilization.

Several groups have shown that EGF stimulus elicits a rapid rise in phosphoinositide and diacylglycerol (DAG) levels in A431 cells (Sawyer and Cohen, 1981; Hepler *et al.*, 1987; Pandiella *et al.*, 1987; Pike and Eakes, 1987; Wahl *et al.*, 1987) and that the tyrosine kinase activity of the EGF-R is required for this response (Moolenaar *et al.*, 1988). Nishizuka (1984) and Berridge and Irvine (1984) reviewed the role of ligand-receptor interactions in the triggering of the hydrolysis of phosphatidylinositol to DAG and inositol 1,4,5-trisphosphate (IP_3) that respectively activate the calcium-dependent protein kinase C (PKC) and release of Ca^{2+} from intracellular stores. Phospholipase C-γ (PLC), which is responsible for the hydrolysis of phosphatidylinositol bisphosphate (PIP_2) to IP_3 and DAG, was shown to be activated by EGF in A431 cells (Wahl *et al.*, 1987, 1989a,b; Margolis *et al.*, 1989; Meisenhelder *et al.*, 1989; Todderud *et al.*, 1990), as well as in other preparations (Kim *et al.*, 1990; Wahl *et al.*, 1990). Additionally, type II phosphatidylinositol kinase was shown to be activated in EGF-stimulated A431 cells (Thompson *et al.*, 1985; Walker and Pike, 1987), and type I was activated in EGF-stimulated NRHER5 fibroblasts (Bjorge *et al.*, 1990).

The mechanism by which intracellular calcium is mobilized is better understood than that by which extracellular Ca^{2+} is transported across the plasma membrane on EGF stimulation. In recent patch-clamp studies using A431 cells, Chapron *et al.* (1989) and Mozhayeva *et al.* (1989) showed that stimulation of the EGF-R with ligand induces a rapid opening of plasma membrane Ca^{2+} channels. The former study indicated that the kinase activity of the EGF-R was necessary to activate the plasma membrane Ca^{2+} channels and that cytosolic IP_3 activated the same channels. Both studies found a lag of a few seconds between EGF addition and activation of Ca^{2+} channel activity; Chapron *et al.* (1989) attributed the lag to ligand diffusion to the cell-attached patch.

PKC is known to phosphorylate threonine 654 on the EGF-R's cytoplasmic side (Cochet *et al.*, 1984; Downward *et al.*, 1984; Hunter *et al.*, 1984). The phosphorylated EGF-R has a lower binding affinity for EGF (Cochet *et al.*, 1984; Fearn and King, 1985). Because PKC is a calcium-dependent enzyme, a rise in $[Ca^{2+}]$ would stimulate PKC activity and, therefore, down-regulate the EGF-Rs on the cell surface. Additionally, it has been suggested that Ca^{2+}-calmodulin regulates EGF-R internalization (Kuppaswamy and Pike, 1989). Thus, one of the roles of a transient rise in $[Ca^{2+}]_i$ may be to begin a negative feedback loop to down-regulate cell surface EGF-Rs and to modulate the effects of EGF on the cell.

In this paper we demonstrate two different types of $[Ca^{2+}]_i$ responses due to EGF stimulation in individual A431 cells. One response, seen at high concentrations of EGF (>4 nM), is a rapid transient increase followed by a sustained elevation of $[Ca^{2+}]_i$ above basal levels. The second, seen at lower concentrations of EGF (1.5 nM), is an oscillation of $[Ca^{2+}]_i$ with no long-term elevation. The response at intermediate EGF concentrations appears to be a kinetic mixture of these two extreme responses. We demonstrate that the kinetics of binding of EGF to EGF-Rs, followed by the cascade of the IP_3 signaling pathway, can predict general features of the kinetics of the onset of the EGF-stimulated $[Ca^{2+}]_i$ response in A431 cells.

Results

Single cell $[Ca^{2+}]_i$ transients

It is generally accepted that one of the earliest responses of serum-starved A431 cells to a challenge with EGF is a transient rise in $[Ca^{2+}]_i$. We have confirmed the report by Gonzalez *et al.* (1988) that a delay occurs between the time cells are exposed to EGF and the onset of a change in $[Ca^{2+}]_i$ and that this lag in response differs from cell to cell. Here we also report individual cell variability in the time course of the change in $[Ca^{2+}]_i$, which is a strong function of [EGF].

We examined EGF-stimulated $[Ca^{2+}]_i$ transients in 191 individual A431 cells on 22 separate cover slips. Cells were exposed to EGF at concentrations of 8.95, 6.95, 4.28, 2.66, 2.02, 1.53, or 0.67 nM. The ligand stimulus was delivered to the cells in a bolus that produced a ligand concentration rise in the bathing solution of ~90% final concentration in <1 s as de-

scribed in Materials and methods. Experiments at [EGF] = 8.95 and 6.95 nM, as well as two experiments at [EGF] = 4.28 nM, were of ~2-min duration with temporal resolution of ~0.8 s between images; the remainder of the experiments was all of ~6-min duration with temporal resolution of ~4 s between images. A summary of the data is given in Table 1.

The lower time resolution data were taken as fura-2 fluorescence image pairs as described in Materials and methods. These data allowed the calibration of $[Ca^{2+}]_i$ for individual cells. For these data, a cell was defined to be responsive when $[Ca^{2+}]_i$ was elevated for ≥25 s to peak levels ≥ 0.25 pCa units above baseline. That is, for a cell with basal $[Ca^{2+}]_i$ of 100 nM, a rise of $[Ca^{2+}]_i$ to >178 nM that occurred over times of 25 s or more was counted as a positive response. The higher time resolution data were taken as single fura-2 images as described in Materials and methods. For these data, a cell was defined to be responsive when the fura-2 signal increased by >5% from its resting level for ≥25 s. In both of the above cases, the initiation of a cellular $[Ca^{2+}]_i$ response was defined as the time point at which $[Ca^{2+}]_i$ began a consistent, monotonic rise that qualified under the above criteria. The response lag time was defined as the time between EGF stimulus and the initiation of the first clear $[Ca^{2+}]_i$ rise in the cell. This lag time was not always well defined for the 2.66- and 2.02-nM data.

Four of 191 cells exhibited prestimulus activity sufficient to qualify as having responded. Two of these 4 (1 in a 4.3-nM stimulus experiment and 1 in a 1.5-nM stimulus experiment) were active before EGF stimulus with a pulsatile rise in $[Ca^{2+}]_i$ followed by a return to baseline; the response of these cells was scored as described above. The 2 remaining cells, in two 1.5-nM stimulus experiments, were active during EGF addition. These cells, even though they showed subsequent activity, were scored as responding with zero lag.

At the highest stimulus levels the fraction of responding cells approached a maximum near 0.7. Decreasing levels of stimulus produced a decrease in the fraction of cells that eventually responded. In consort with the decrease in cell response was an increase in the mean lag time between stimulus and response. The variability of the lag time from cell to cell also increased with decreasing dose, as is reflected in the standard deviation of the mean lag time in Table 1. This variability from cell to cell and increase in mean lag time with decreasing [EGF] are also seen in a plot of the fraction of cells responding versus time of response (Figure 1). The response of a population of cells is seen to be more rapid at high [EGF] and slower at low [EGF].

The details of the time-dependent behavior of the individual cell $[Ca^{2+}]_i$ responses varied from cell to cell and were strongly dependent

Table 1. Summary of cell responses

[EGF] (nM)	Total # cells tested	Fraction of cells responding	Average resting pCa	Average peak pCa	Average elevated pCa	Mean lag time (s)	Lag time range (s)
8.95[a]	18	0.67	6.74 ± 0.10	ND[b]	ND	6.6 ± 1.4	5–9
6.95	25	0.72	6.81 ± 0.12	ND	ND	10.5 ± 4.5	5–20
4.28[c]	36	0.58	6.90 ± 0.25	6.16 ± 0.38	6.79 ± 0.09	15.9 ± 9.9	8–32
2.66	23	0.48	6.98 ± 0.11	6.53 ± 0.13	6.76 ± 0.15	37.6 ± 15.8	22–62
2.02	32	0.44	7.30 ± 0.07	6.72 ± 0.20	7.13 ± 0.07	78.5 ± 116	7–348
1.53	44	0.39	6.82 ± 0.29	6.19 ± 0.50	none	162.4 ± 128	0–408[d]
0.67	13	0.00	6.77 ± 0.12	none	none	none	none

[a] These experiments were performed without ratio imaging to improve temporal resolution. The resting pCa for these experiments was determined from a single 334/365-nm image pair at the start of each image collection sequence.

[b] Not done.

[c] For this stimulus level, 23 cells were examined using ratio imaging, and 13 cells were examined without ratio imaging. The resting pCa levels for the latter 13 cells were determined from a single 334/365 ratio image pair at the start of each image collection sequence and were averaged with those of the 23 other cells. The peak and elevated pCa values were determined only for the cells responding during ratio imaging.

[d] Two cells responding before and during EGF challenge were scored with zero lag. The next cell to respond did so with a 20-s lag time.

A431 cells were exposed to EGF at various concentrations, and the time course of $[Ca^{2+}]_i$ response of individual cells was measured as described in Materials and methods. The resting pCa, peak pCa, postpeak elevated pCa, and lag time between stimulus and response initiation were measured.

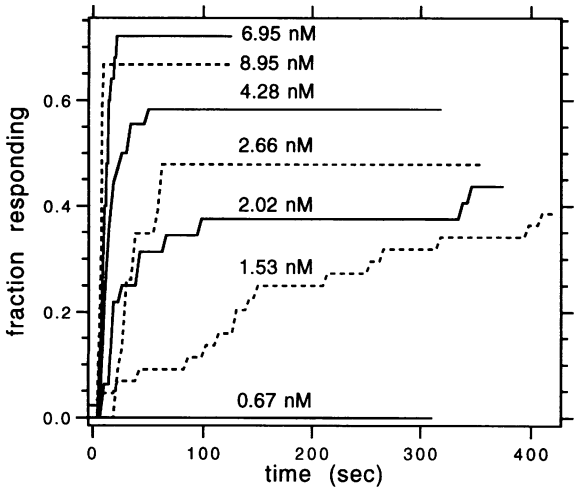

Figure 1. **The fraction of A431 cells responding to seven different concentrations of EGF are plotted vs. time.** Individual cell response is scored as noted in the text.

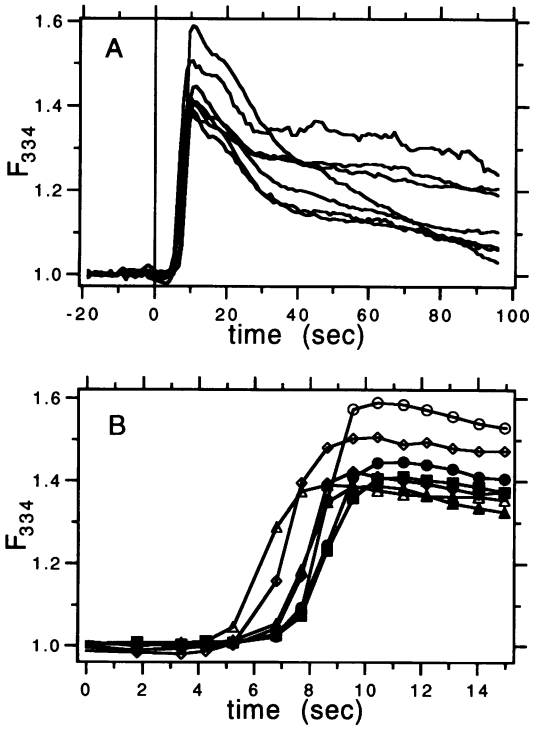

Figure 2. **Time course of response of seven A431 cells to 8.95 nM EGF added at t = 0 s.** The fura-2 response was recorded only at 334 nm excitation to increase temporal resolution. All individual cell fluorescence levels before stimulus were normalized to unity. Seven cells were in the field of view. (A) Full time course of the experiment. (B) Expanded time course.

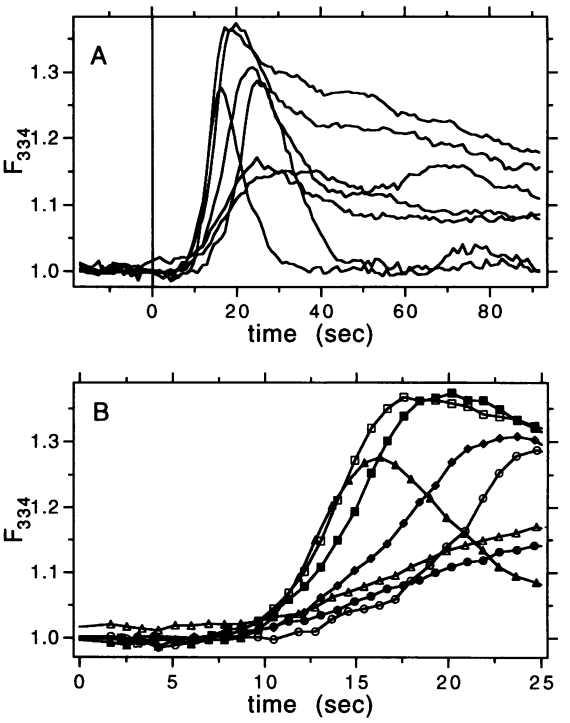

Figure 3. **Time course of response of seven A431 cells to 6.95 nM EGF added at t = 0 s.** The fura-2 response was recorded only at 334 nm excitation to increase temporal resolution. All individual cell fluorescence levels before stimulus were normalized to unity. Seven cells from two experiments are shown. (A) Full time course of the experiment. (B) Expanded time course.

on the level of EGF stimulus. For the three highest levels of stimulus, 9.0, 7.0, and 4.3 nM, $[Ca^{2+}]_i$ rose rapidly after a 5- to 32-s lag and subsequently decayed to a level persistently elevated above basal for most responding cells (Figures 2–4). The lag time between stimulus and response clearly varied from cell to cell and the duration of the initial rising phase of the $[Ca^{2+}]_i$ response was about the same as the lag that preceded it for most cells (Figures 2B and 3B). Because the 9.0- and 7.0-nM data were taken with fura-2 excitation only at 334 nm, the relative $[Ca^{2+}]_i$ levels during the response were not computed. For the 4.3-nM EGF stimulus, responding cells displayed mean peak $[Ca^{2+}]_i$ 7.6 times greater than mean basal levels (91 nM) followed by a persistent elevation 1.8-fold above basal $[Ca^{2+}]_i$.

No response was found in cells treated with 0.67 nM of EGF (Figure 5) for up to 5 min. Cells challenged with 1.53 nM of EGF displayed pseudoperiodic oscillations rising and falling from basal $[Ca^{2+}]_i$ levels (Figure 6). For the latter level of stimulus, the lag time between EGF ad-

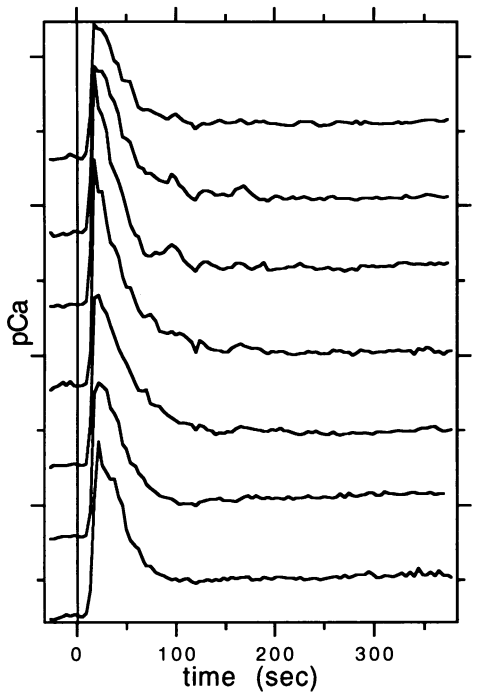

Figure 4. **Response of seven A431 cells to 4.28 nM EGF added at t = 0 s.** Individual cell responses are vertically offset by 0.5-pCa units for clarity. Large tic marks on the vertical axis are spaced at 1.0-pCa units. There were 10 cells in the field of view.

dition and initiation of the first rise in $[Ca^{2+}]_i$ ranged up to 408 s. The mean oscillation peak height was 4.3-fold elevated over basal $[Ca^{2+}]_i$. The oscillations were asynchronous from cell to cell and were in some cases of limited duration.

The time course of $[Ca^{2+}]_i$ responses to EGF stimulus levels of 2.02 and 2.66 nM appeared to be a mix of the spike plus persistent elevation seen in Figures 2–4 and the oscillations seen in Figure 6. At 2.7-nM EGF stimulus, the lag times varied from 22 to 62 s (Figure 7, Table 1). Most cells that responded at this level of stimulus showed an initial peak with onset kinetics noticeably slower than found with 4.3 nM stimulation (Figure 4); the mean peak was 2.8-fold elevated over basal $[Ca^{2+}]_i$. Some cells displayed subsequent $[Ca^{2+}]_i$ oscillations reminiscent of those found at lower stimulus levels (Figure 6) except that they appeared less robust, of lesser duration, and superimposed on an elevation ~ 1.7-fold above basal $[Ca^{2+}]_i$.

A challenge with 2.0 nM of EGF brought about varied delay in cell response greater than that for 2.7 nM of stimulation (Table 1, Figure 8). The kinetic response was more similar to the oscillations found at 1.5 nM of stimulation than the spike plus persistent elevation found at 4.3 nM. A low-amplitude component of an initial rise followed by a persistent elevation ~ 1.5-fold over basal $[Ca^{2+}]_i$ was seen in some cells (Figure 7), whereas "oscillations" were isolated or of much longer period as compared with those produced by 1.5 nM of stimulation (Figure 6). Average peak $[Ca^{2+}]_i$ was 3.8-fold elevated over mean basal levels.

For all of the cells described above, the fraction of cells responding and the mean lag time for responding cells were compared with the degree of cell to cell contact because A431 cells grow in clumps. The degree of contact was crudely assayed as the fraction of a cell's periphery in contact with other cells on the basis of the fura-2 images of the cells. No obvious correlation between the fraction of cells responding and degree of cell contact was observed (Table 2), although the lag time between stimulus and response was somewhat correlated. Increasing lag times at a particular dose level were found, on average, to increase with cell to cell contact.

For a particular responding cell, the lag time between stimulus and response and the rise time from the initiation of the response to the peak of the response were not strongly corre-

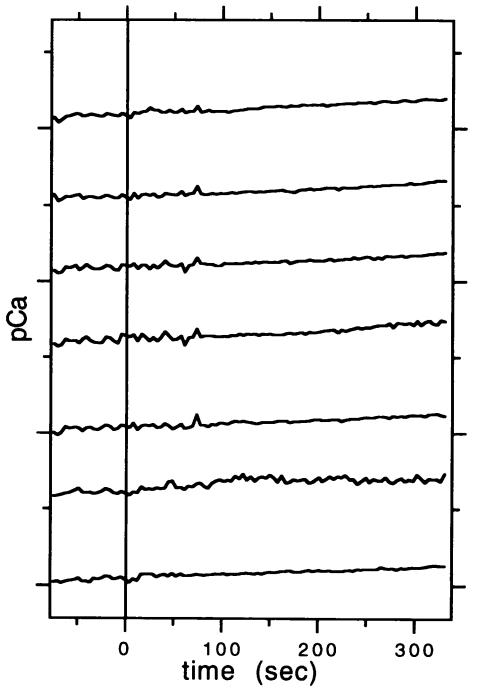

Figure 5. **Response of seven A431 cells to 0.67 nM EGF added at t = 0 s.** Individual cell responses are vertically offset by 0.5-pCa units for clarity. Large tic marks on the vertical axis are spaced at 1.0-pCa units. There were seven cells in the field of view.

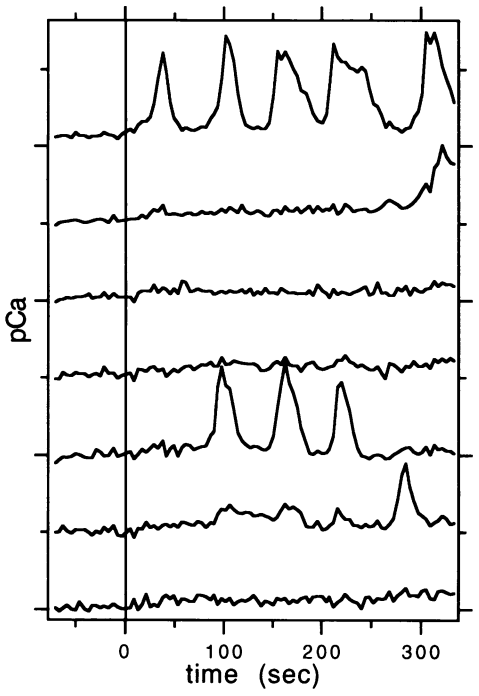

Figure 6. **Response of seven A431 cells to 1.53 nM EGF added at t = 0 s.** Individual cell responses are vertically offset by 0.5-pCa units for clarity. Large tic marks on the vertical axis are spaced at 1.0-pCa units. There were seven cells in the field of view.

lated (Figure 9). For all but three cells, the rise time of the EGF-induced $[Ca^{2+}]_i$ response was under 100 s. However, for many cells, all at [EGF] of 2.02 and 1.53 nM, the lag time was very long compared with the rise time. For cells responding within 30 s of EGF challenge, the rise time of the $[Ca^{2+}]_i$ response was roughly linear with the lag time (Figure 9, inset), although the linear regression correlation coefficient for these data was only 0.7. A minimal lag time of ~5 s is seen in the data of Figure 9. Data from two cells exhibiting activity before and during EGF addition, for which the lag time was scored as 0 s, have not been included in this figure.

A simple model of response initiation kinetics

To explore the role of the EGF-stimulated enzyme cascade in the generation of the lag between stimulus and $[Ca^{2+}]_i$ responses described above, a simple kinetic model was studied. As all $[Ca^{2+}]_i$ transients are in response to ligand challenge, the initial step in the model is EGF binding to the EGF-R. This is followed by activation of PLC, production of IP_3, and release or influx of Ca^{2+}. All reactions after ligand binding to receptor are considered to be portions of a catalytic cascade, and these reactions are assumed to be rate limited only by the amount of enzyme present. The latter assumption implies that all reactions subsequent to ligand binding are assumed to occur with little consumption of substrate (PLC or PIP_2) or with little discharge of the IP_3-sensitive Ca^{2+} stores. Additionally, degradative or desensitizing pathways that inactivate the EGF/EGF-R complex, activated PLC or IP_3 are assumed to be slow relative to the time course of the initiation of the $[Ca^{2+}]_i$ response. Thus, this model addresses only the time dependence of the initiation of a ligand-activated $[Ca^{2+}]_i$ response.

Because the EGF/EGF-R interaction is monovalent (Lax *et al.*, 1990), the equation describing the time dependence of the formation of EGF/EGF-R complexes is

$$d[ER]/dt = k_f[E][R] - k_r[ER] \qquad (1)$$

In Eq. *1* k_f and k_r stand for the forward and reverse rate constants of ligand-receptor binding, whereas ER, E, and R represent the EGF/EGF-R complex, free EGF, and unbound EGF-R, respectively. The latter three parameters are all

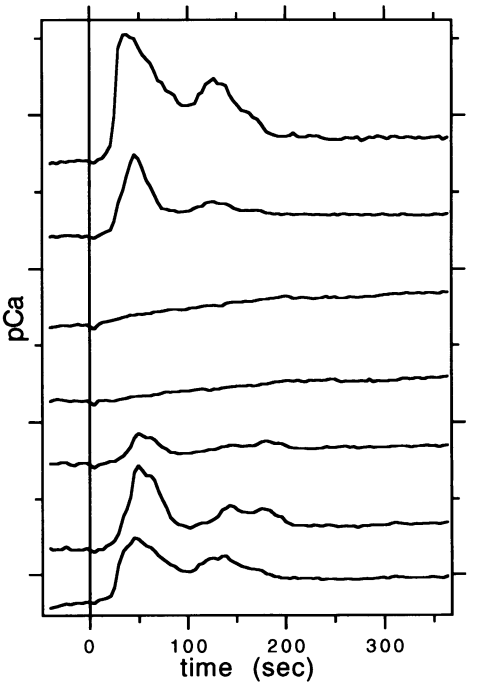

Figure 7. **Response of seven A431 cells to 2.66 nM EGF added at t = 0 s.** Individual cell responses are vertically offset by 0.5-pCa units for clarity. Large tic marks on the vertical axis are spaced at 1.0-pCa units. There were 12 cells in the field of view.

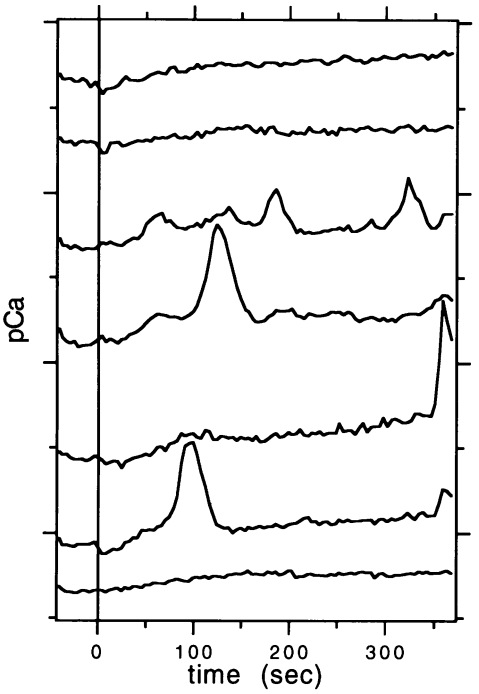

Figure 8. **Response of seven A431 cells to 2.02 nM EGF added at t = 0 s.** Individual cell responses are vertically offset by 0.5-pCa units for clarity. Large tic marks on the vertical axis are spaced at 1.0-pCa units. There were 12 cells in the field of view.

time dependent. As low- and high-affinity interactions of EGF with the EGF-R have different kinetic reaction rates (Bellot *et al.,* 1990), both types of interaction are included in the model.

The final step in the model is IP_3-mediated release of calcium from intracellular stores and/or IP_3-mediated opening of plasma membrane calcium channels (Pandiella *et al.,* 1987; Chapron *et al.,* 1989). In either case, a rise in $[IP_3]$ initiates a concomitant rise in $[Ca^{2+}]_i$, the quantity of interest. Intermediate steps involve activation of PLC and conversion of PIP_2 to DAG and IP_3. Because PLC activation is catalyzed by activated EGF-R as noted in the Introduction

$$d[PLC^*]/dt = K_P[ER] \quad (2)$$

where PLC* indicates the activated form of PLC and K_P is an effective rate constant containing information about the total PLC concentration, the affinity of PLC for ER, and the catalytic conversion efficiency of the activated EGF-R. Likewise, with similar assumptions, the rate of IP_3 production is

$$d[IP_3]/dt = K_I[PLC^*] \quad (3)$$

and the rate of release of calcium from stores or influx from the extracellular milieu is

$$d[Ca^{2+}]_i/dt = K_C[IP_3]^3 \quad (4)$$

where K_I and K_C are constants similar to K_P in Eq. *2* and where IP_3 acts on its receptor cooperatively, with a valence of ~3 (Meyer *et al.,* 1988). We assume this valence also applies to the plasma membrane IP_3-gated channels.

This model is formally equivalent to a three-step unidirectional cascade (Stadtman and Chock, 1979), which, as noted by Chock *et al.* (1980), produces a high degree of signal ampli-

Table 2. Response vs. portion of cell periphery in contact with other cells

	<0.25			0.25–0.50			0.50–0.75			>0.75		
[EGF] (nM)	Total # cells	Fraction responding	Mean lag (s)	Total # cells	Fraction responding	Mean lag (s)	Total # cells	Fraction responding	Mean lag (s)	Total # cells	Fraction responding	Mean lag (s)
8.95	1	1.00	7	5	1.00	5 ± 1	7	0.57	7 ± 2	5	0.47	7 ± 1
6.95	1	1.00	9	5	0.80	8 ± 4	12	0.50	11 ± 4	7	0.71	12 ± 6
4.28	4	0.25	10	9	0.67	11 ± 2	19	0.57	17 ± 9	4	0.75	24 ± 20
2.66	1	0.00	—	6	0.67	37 ± 16	10	0.20	51 ± 16	6	0.33	24 ± 3
2.02	3	0.33	22	7	0.29	14 ± 10	14	0.50	91 ± 117	8	0.38	132 ± 183
1.53	2	1.00	162 ± 51	10	0.40	181 ± 175	20	0.35	123 ± 116	12	0.50	237 ± 145
0.67	0	—	—	5	0.00	—	5	0.00	—	3	0.00	—
Total, all [EGF]	12	0.50		47	0.53		87	0.45		45	0.42	

As described in Materials and methods, the time course of $[Ca^{2+}]_i$ changes in A431 cells responding to EGF was measured. The responses of individual cells were characterized with respect to the degree of contact with other cells. Cells were separated into four categories (<0.25, 0.25–0.50, 0.50–0.75, and >0.75), given the apparanet fraction of peripheral membrane contact with other cells. This measure is qualitative because the true extent of membrane contact cannot be ascertained with the limited resolution of the optical microscope. In each category, the total number of cells, fraction of cells responding, and mean (±SD) lag time between stimulus and response are given for each EGF dose level.

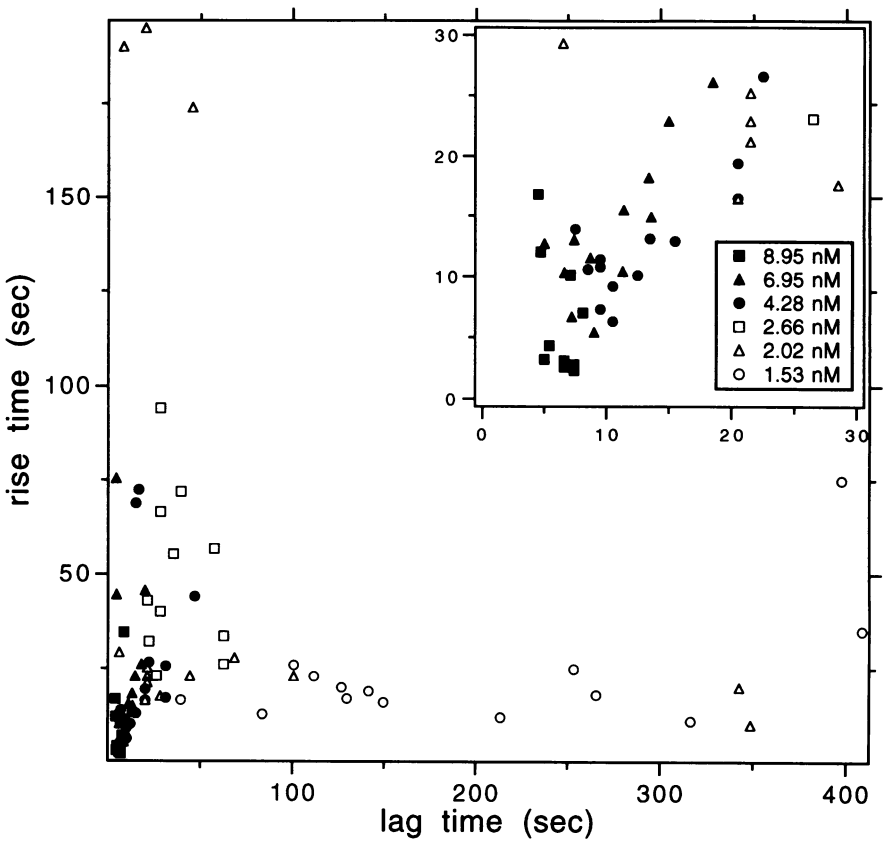

Figure 9. **Rise time of individual cell $[Ca^{2+}]_i$ responses vs. lag time of response for various [EGF] as indicated in the figure.** Inset, the data for lag and rise times < 30 s.

fication accompanied by a lag between stimulus and response. Under our assumptions, the cell acts as a signal integrator, accumulating signal (i.e., $[Ca^{2+}]_i$) over time.

To test the model, numerical solutions to Eq. *1* were computed for step changes of [EGF]. Rate constants for EGF binding to the high- and low-affinity states of the EGF-R were assumed to be $k_{f,hi} = 9.8 \times 10^6\ M^{-1}s^{-1}$, $k_{r,hi} = k_{r,lo} = 2.9 \times 10^{-3}\ s^{-1}$, and $k_{f,lo} = 2.5 \times 10^5\ M^{-1}s^{-1}$ (Bellot *et al.,* 1990). Thus, the dissociation constant for the high-affinity state of the EGF-R, $K_{d,hi}$, is 0.3 nM, whereas that for the low-affinity state, $K_{d,lo}$, is 12 nM. These values are from bulk cell studies and thus could be different for a particular cell. From the imaging experiments described above, we estimate that 4×10^4 cells are exposed to EGF in the 800-μl volume of the flow chamber. As A431 cells express about 2×10^6 EGF-R per cell ($\sim 5 \times 10^5$ of these are in the high-affinity state) (Defize *et al.,* 1988; although see Kawamoto *et al.,* 1983), a total of 8×10^{10} receptors are present to remove EGF from the medium in the flow chamber. The numerical solutions include depletion of EGF from the medium by this mechanism.

Because the rate constants in Eqs. *2–4* were not known, only the qualitative aspects of the signaling cascade kinetic model were characterized. Numerical solutions to Eqs. *1–4* were computed for each [EGF] used above (see Table 1). Two separate cases were considered, one in which both high- and low-affinity receptors activated PLC and one in which only the high-affinity class was active. The value of the model-predicted $[Ca^{2+}]_i$ signal was normalized to the value of the signal at [EGF] = 8.95 nM and t = 6.6 s, the mean lag time for this level of stimulus as measured (Table 1). This $[Ca^{2+}]_i$ level corresponds to the value of $[Ca^{2+}]_i$ at which a cell begins to respond, and the time at which this level is reached is the predicted lag time. Although this reference level differed markedly for simulations with both receptor affinity classes active and only high-affinity receptors active, the predicted relative lag times at the different EGF levels were not significantly different for these two cases (not shown). The values predicted by the simulation with high-affinity receptors are shown in the far left column of Table 3. This simple model predicts lag times that increase with decreasing dose but that are

Table 3. Lag time predictions from a signal cascade model

[EGF] (nM)	Model lag time (s)											
	$k_d = 0\ s^{-1}$			$k_d = 1\ s^{-1}$			$k_d = 10\ s^{-1}$			$k_d = 100\ s^{-1}$		
	0[a]	10[a]	100[a]	0[a]	10[a]	100[a]	0[a]	10[a]	100[a]	0[a]	10[a]	100[a]
8.95	6.6	6.6	6.6	6.6	6.6	6.6	6.6	6.6	6.6	6.6	6.6	6.6
6.95	7.1	7.3	7.3	7.2	7.7	7.7	7.3	7.8	7.9	7.3	7.9	7.9
4.28	8.1	8.8	8.8	8.6	10.4	10.4	8.8	11.0	11.1	8.8	11.1	11.1
2.66	9.3	10.7	10.7	10.2	14.2	14.3	10.7	15.4	15.5	10.7	15.5	15.6
2.02	10.0	12.0	12.0	11.4	17.1	17.2	12.0	18.7	18.9	12.0	18.9	19.0
1.53	10.9	13.4	13.5	12.7	20.6	20.8	13.4	22.9	23.1	13.5	32.1	23.2
0.67	13.9	18.9	19.1	17.5	36.9	37.3	18.8	41.5	41.9	19.0	42.0	42.4

Predicted lag times of the EGF-stimulated $[Ca^{2+}]_i$ response for various combinations of receptor desensitization and IP_3 removal constants. The responses in each vertical column were normalized to the value at [EGF] = 8.95 nM for t = 6.6 sec.
[a] k_{con} (s^{-1}).

shorter than measured values for [EGF] < 8.95 nM (Tables 1 and 3). Because no mechanism for attenuation of any step in the signaling pathway is included in Eqs. *2–4,* the model predicts a rise in $[Ca^{2+}]_i$ that increases without bound. In the cell, Ca^{2+} pumps, Ca^{2+} binding proteins, and other signal attenuation mechanisms would act to prevent the unbounded rise in $[Ca^{2+}]_i$ or in other constituents of the signaling pathways. Additionally, desensitization of the EGF receptor would also dramatically reduce the propagation of second messenger signals because receptor activation begins the signal cascade sequence.

The effects of both desensitization of active receptors and constitutive removal of IP_3 were examined by including in Eqs. *1* and *3* rate constants k_d and k_{con} that allowed removal of active receptors and/or IP_3 from the model system. Equations *1* and *3* thus become

$$d[ER]/dt = k_f[E][R] - k_r[ER] - k_d[ER]$$

and

$$d[IP_3]/dt = K_l[PLC] - k_{con}[IP_3] \qquad (5)$$

The numerical solutions to Eqs. *2, 4,* and *5* for various values of k_d and k_{con} were computed for the case in which high-affinity receptors were the active receptor species. The predicted lag times are shown in Table 3. For all simulations the predicted lag times increase with decreasing [EGF], but all are shorter than measured values. We interpret this finding as an indication that constitutive or stimulated signal attenuation mechanisms are important even for times as short as 5 s after stimulus, and that signal attenuation beyond receptor desensitization and IP_3 removal plays a major role in the initiation kinetics for the low-dose EGF stimuli.

This very simple model predicts the lag followed by a rapid increase in $[Ca^{2+}]_i$, as seen experimentally. Figure 10 shows the predicted increase of $[Ca^{2+}]_i$ for $k_d = 1\ s^{-1}$, $k_{con} = 10\ s^{-1}$, and other rate constants as described above. The predicted rise in $[Ca^{2+}]_i$ is seen to be most rapid at [EGF] = 8.95 nM. This rate of rise diminishes with decreasing [EGF].

For the values of $k_d = 1\ s^{-1}$ and $k_{con} = 10\ s^{-1}$, the effect of changing the number of receptors on a cell by ±50% was computed. Increasing the net number of high-affinity receptors by 50% from 1.0×10^5 to 1.5×10^5 decreased the predicted lag times by 25%, whereas decreasing the receptor number to 0.5×10^5 increased the predicted lag time by 74%. Thus, this simple model predicts a wide variation in individual cell response times with variation in receptor number.

Discussion

We have shown that stimulation of A431 cells with EGF in the concentration range 8.95–0.67 nM produces characteristic kinetics of changes in $[Ca^{2+}]_i$ that vary dramatically, particularly over the stimulus concentration range 4.5–1 nM. High-dose levels produce a transient spike increase in $[Ca^{2+}]_i$ that decays to a persistently elevated level. Low-dose levels produce an oscillatory $[Ca^{2+}]_i$ response, whereas [EGF] below 1 nM produces no response. A decrease in EGF dose level produces an increase in the delay (lag) between stimulus and $[Ca^{2+}]_i$ response for cells that respond.

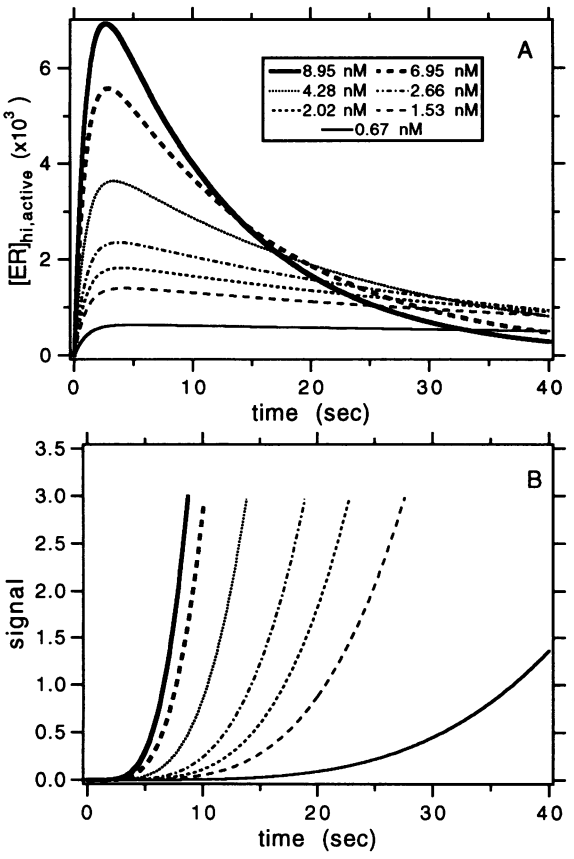

Figure 10. **Signal cascade model predictions when only high-affinity receptors contributed to the initiation of the signal with desensitization of active receptors and removal of IP_3.** (A) Time course of changes in active receptor number. (B) Time course of the initiation of a $[Ca^{2+}]_i$ response (signal).

Our data correspond well to those of several other groups (Moolenaar *et al.*, 1986; Hepler *et al.*, 1987; Pandiella *et al.*, 1987; Gonzalez *et al.*, 1988) in clearly demonstrating that stimulus with high (5–10 nM) [EGF] brings about a rapid rise in free cytosolic $[Ca^{2+}]$ after agonist introduction, with a high amplitude spike followed by a prolonged elevation in cytosolic $[Ca^{2+}]$ above resting levels. Although we did not test for the release of Ca^{2+} from internal stores using Ca^{2+}-free medium, we can compare our data from low and high [EGF] experiments to those of Pandiella *et al.* (1987) and Hepler *et al.* (1987), where high [EGF] and Ca^{2+}-free or Ca^{2+}-containing media were used. Both groups observed that A431 cells in Ca^{2+}-free medium showed a response to high levels of EGF with a shorter $[Ca^{2+}]$ transient of lower amplitude than those cells challenged in Ca^{2+}-containing medium. Also, both studies showed that cells in Ca^{2+}-free medium did not show a persistent rise in cytosolic $[Ca^{2+}]$ after the initial transient, whereas cells in Ca^{2+}-containing medium did exhibit a prolonged elevation of $[Ca^{2+}]$. We found that the transients induced at low [EGF] were of shorter duration than those stimulated by higher agonist concentrations and were not followed by a prolonged elevation of cytosolic $[Ca^{2+}]$ above resting levels. Thus, the shape of the EGF-stimulated Ca^{2+} transient is regulated both by agonist concentration and the concentration of Ca^{2+} in the medium. These results suggest that activation of plasma membrane calcium channels may produce the long duration elevation of $[Ca^{2+}]_i$ at high doses of EGF and that EGF-activated plasma membrane Ca^{2+} channels play little or no role in the $[Ca^{2+}]_i$ response to low EGF doses.

The EGF-stimulated $[Ca^{2+}]_i$ response, from maximal to none, of individual A431 cells contrasts sharply with the responses of individual hepatocytes to vasopressin stimulus (Woods *et al.*, 1986; Rooney *et al.*, 1989) or of endothelial cells to histamine stimulus (Jacob *et al.*, 1988). For these cells and stimuli, $[Ca^{2+}]_i$ oscillations increase in frequency with increasing stimulus level until the oscillations "fuse" into a sustained, markedly elevated level of $[Ca^{2+}]$. This gradation of response occurs over an order of magnitude of stimulant concentration. In contrast, EGF-stimulated oscillations in A431 cells are found only over a very narrow [EGF] range. Further, a second distinct $[Ca^{2+}]_i$ response to EGF stimulation is seen: an isolated spike of $[Ca^{2+}]_i$ followed by a sustained elevation above initial basal levels. Stimulus with 2.0 and 2.7 nM EGF induced $[Ca^{2+}]_i$ responses that were an admixture of these two distinct response patterns. These results indicate that for A431 cells and EGF stimulus, the $[Ca^{2+}]_i$ response may be regulated by two separate control pathways. One possible pair of Ca^{2+} regulatory pathways in A431 cells is the IP_3-activated release from intracellular stores and influx through plasma membrane channels. Differential regulation of these two Ca^{2+} pathways could be readily accomplished because they are spatially separate.

We have examined a simple model of the initiation of these complex $[Ca^{2+}]_i$ responses in EGF-stimulated A431 cells. The primary signal of EGF binding to its receptor is transduced and amplified through the known cascade of enzymatic steps leading to the release of Ca^{2+} from IP_3-sensitive stores or influx of Ca^{2+} from the extracellular milieu through IP_3-sensitive plasma membrane channels. Such a catalytic cascade signal pathway leads to a $[Ca^{2+}]_i$ signal with a prolonged lag phase subsequent to stimulus

followed by a sharp increase. This model contrasts with other signal initiation models of delayed K^+ current activated by acetylcholine stimulus of heart muscle cells (Marty *et al.*, 1989) and of $[Ca^{2+}]_i$ responses in the context of the Ca^{2+}-induced Ca^{2+} release model of $[Ca^{2+}]_i$ oscillations (Dupont *et al.*, 1990). The former model assumes stoichiometric interactions between activated receptors, G-proteins, and plasma membrane K^+ channels. In the same paper, Marty *et al.* (1989) discussed the acetylcholine-stimulated release of Ca^{2+} in rat lacrimal cells, for which they suggested a model similar to that examined here, with the exception that activated receptors, G-proteins, and PLC are considered to react together stoichiometrically rather than enzymatically. Marty *et al.* (1989) did not develop this model further, but rather suggested that response lag times are due to the formation of microdomains of IP_3 produced in the vicinity of active PLC molecules. From our analysis, this assumption appears to be unnecessary as the cascade of enzymatic reactions can account for both the delay of and the explosive increase in the delivered signal.

In the model by Dupont *et al.* (1990), all of the factors in the signal cascade model up to the point of stimulation of Ca^{2+} release by IP_3 are contained in a parameter β that is presumed to increase as a step function or as an exponential after ligand challenge. Such an exponential rise in $[IP_3]$ was predicted by Miledi and Parker (1989) for low-level serum stimulus of *Xenopus* oocytes. The enzymatic cascade model that we analyzed predicts a very different time course of IP_3 production, namely, one similar to but not as pronounced as the predicted lag followed by explosive increase in $[Ca^{2+}]_i$, as shown in Figure 10B.

We explored three variations of the signal cascade model to better understand its properties. First, the inclusion of constitutive degradation of IP_3 similar to that proposed by Parker and Miledi (1986) decreased the amplitude of the $[Ca^{2+}]_i$ signal at any particular stimulus level and also increased the relative lag time for low doses of EGF (Table 3). We found that this relative increase in lag time was not much enhanced for values of the constitutive rate constant k_{con} beyond 10 s^{-1} and that the predicted lag times were shorter than the measured lag times, particularly for low [EGF]. Thus, constitutive loss of IP_3 cannot alone account for measured lack of response of A431 cells to 0.67 nM EGF or for the very long lag times found for 2.7–1.5 nM stimuli. The second variation of the basic model, desensitization of the active liganded receptor, produced similar results. These two variations in combination produced much longer lag times, particularly for the lower EGF concentrations. This simple model, based on the known enzymatic cascade initiated by EGF binding to its receptor, predicted a lag phase followed by a sharp increase in $[Ca^{2+}]_i$ as well as variability from cell to cell based on variation in the numbers of EGF receptors on a cell. However, the lag times predicted by the model remained shorter than measured values. Clearly, other constitutive or stimulated attenuation mechanisms for calcium ions and other signaling molecules must operate to reduce the rate of accumulation of signal in A431 cells. An additional complication for the case of EGF receptors on A431 cells that we have not considered is the anomalous diffusion-limited binding of EGF due to high cell surface receptor density (Wiley, 1988).

The third variation of the basic model explored the relative efficacy of high-affinity and low-affinity receptors to initiate a $[Ca^{2+}]_i$ response. Qualitatively, both receptor classes gave identical results, although high-affinity receptors produced quantitatively more abrupt increases in $[Ca^{2+}]_i$. The lack of significant differences in model predictions between low- and high-affinity receptors primarily is due to the fact that responses are relative to the response of a particular model case for [EGF] = 8.95 nM. With no receptor desensitization or IP_3 removal, either class of receptor is capable of generating similar $[Ca^{2+}]_i$ responses. Other studies employing monoclonal antibodies specific for either the low- or high-affinity EGF-R subtypes have shown that the high-affinity receptor is the dominant primary signal transducer in A431 and EGF-R-transfected NIH 3T3 cells (Defize *et al.*, 1989; Bellot *et al.*, 1990). This is consistent with the predictions of the simple enzymatic signal cascade analysis presented here.

Materials and methods

Cells and flow chamber preparations

Human epidermoid carcinoma A431 cells were obtained from Leon Heppel, Cornell University, Ithaca, NY. The cells were grown in 75-cm^2 flasks in Dulbecco's modified Eagle's medium (DMEM; GIBCO, Grand Island, NY), supplemented with 10% (vol/vol) fetal calf serum in a 37°C, 5% CO_2/95% air humidified atmosphere. Cells for experiments were plated on #1 glass coverslips in individual 35-cm^2 petri dishes at 7.5×10^4 cells per dish. The cells were further incubated for 3–4 d. Seventeen to 24 h before use the cover slips were rinsed in DMEM alone, placed into new individual petri dishes containing 2 ml of unsupplemented DMEM, and incubated as above.

Thirty minutes before use the cells were loaded with the calcium-sensitive dye fura-2 by incubation at 37°C with the

acetoxymethyl ester of fura-2 (fura-2/AM; Molecular Probes, Eugene, OR). Fura-2/AM in a 1-mM stock solution in dry dimethyl sulfoxide (DMSO) was mixed with the DMEM in the petri dish to a final concentration of 2 μM fura-2/AM and 0.2% DMSO. After incubation the cells were rinsed twice in *N*-2-hydroxyethylpiperazine-*N'*-2-ethanesulfonic acid (HEPES)-buffered saline (HBS: 10 mM HEPES, 140 mM NaCl, 5 mM KCl, 1 mM $CaCl_2$, 1 mM $MgCl_2$, 10 mM α-D-glucose, pH 7.4) and mounted in a flow-through chamber, as previously described by Linderman *et al.* (1990).

Once a coverslip was secured in the flow chamber, the chamber was filled with HBS and mounted on the microscope stage for immediate viewing. The stage and microscope objective were kept at 37°C as previously described (Linderman *et al.*, 1990).

Preparation of agonist and introduction into flow chamber

Receptor-grade murine EGF was purchased from Collaborative Research (Bedford, MA). EGF solutions were made by serial dilution from a stock solution of 16.5 μM EGF. Actual concentrations of EGF in the cell stimulus solutions were assayed by a sandwich enzyme-linked immunosorbent assay. In this assay, anti-mouse-EGF rabbit antiserum (Bioproducts for Science, Indianapolis, IN) was adsorbed to multiwell plates (Dynatech Lab, Chantilly, VA), and aliquots of the EGF solutions were added to different wells. The wells were rinsed, and biotinylated anti-mouse-EGF antiserum was added. The antiserum was biotinylated by standard procedures with biotin *N*-hydroxysuccinimide ester (Molecular Probes). After a rinse, avidin-peroxidase (Sigma Chemical Co., St. Louis, MO) was bound to the wells. Peroxidase activity was assayed with peroxide and 3,3',5,5'-tetramethylbenzidine (Kirkegaard and Perry Lab, Inc., Gaithersburg, MD) using a Vmax plate reader (Molecular Devices, Palo Alto, CA). The assays were repeated with 2 mg/ml bovine serum albumin added to the EGF solutions as a blocking agent for nonspecific binding sites. Analysis of the data indicated the presence in our apparatus of binding sites of a single, low affinity (not shown). The concentrations of EGF reported in Results are computed from this analysis.

EGF was introduced into the flow chamber by an injection of ~1.5 ml of stimulus buffer, typically within 40–80 s after the first image frame in a time-lapse sequence. The time course of solution addition was measured by injecting a solution of fluorescein in HBS into the chamber under conditions identical to those for EGF addition (Figure 11). Solution exchange was 95% efficient and most of it occurred over a time course of <2 s. For analysis of the timing of cellular $[Ca^{2+}]_i$ responses, the time of EGF stimulus was defined as the time at which [EGF] was ~50% of its final concentration, i.e., 0.5 s after EGF addition.

Instrumentation

The fluorescence epi-illumination system employed a 75-W Hg-Xe arc lamp (Hamamatsu Corp., Bridgewater, NJ) and a pair of monochromators (model H20, Instruments SA, Inc., Metuchen, NJ). One monochromator was set for center wavelength of 365 nm and the other for 334 nm; thus, fura-2 was excited at the two wavelengths that correspond to spectral lines of the Hg-Xe arc. The exit port of each monochromator was coupled with one of the two ends of a bifurcated quartz fiber optic bundle (Volpi Manufacturing USA, Auburn, NY). This bundle terminated with a circular cross section that directed the fluorescence excitation light through a computer-controlled electronic shutter (A.W. Vincent Associates, Inc., Rochester, NY). The light then passed through a fused silica biconvex lens into the epi-illumination port of a Zeiss IM-35 inverted microscope (Carl Zeiss, Inc., Thornwood, NY) that was equipped with quartz epi-illumination optics and a Nikon 40×/1.3 NA CF Fluor UV lens (Nikon, Inc. Instrument Division, Garden City, NJ). Images were detected by a charge coupled device (CCD) instrumentation camera (Photometrics, Ltd., Tucson, AZ). The imaging system was computer-controlled by a Masscomp 5550 computer (Concurrent Computer Corp., Tinton Falls, NJ).

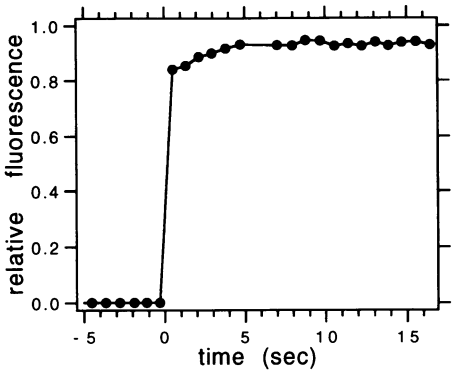

Figure 11. **Time course of solution exchange in the cell chamber.** A standard volume (1.5 ml) of fluorescein solution was added by manual injection at t = 0 s.

Image collection and CCD operation

Most of the data presented here were collected with the CCD operating in frame transfer mode. In this mode the CCD acted as both a photoelectron storage device as well as a collection device. Half the microscope viewing field was masked by a partial field stop. The image in the visible half of the field was collected by illumination at 365 nm for 50 ms. This image was electronically shifted to the masked half of the CCD chip in under 1 ms (Linderman *et al.*, 1990). A second image of the same half of the field was then taken at 334 nm excitation for 500 ms. The final CCD image shows the same field twice, once for each wavelength. All frame transfer images were binned 2 × 2, such that photoelectrons of two pixels in the x direction and two pixels in the y direction were combined to form one large pixel. These data images were collected sequentially every 4 s.

High time resolution fura-2 images were taken with a single exposure of 50 ms at 334 nm excitation. Binning the images 8 × 8 allowed the shorter exposure time and permitted sequential image collection every 0.8 s.

Image collection and processing were accomplished through a menu-driven software package, heavily modified from a base system, Paragon-IPS (Paragon Imaging, Inc., Lowell, MA), that has been described elsewhere (Linderman *et al.*, 1990).

Image processing and data analysis

For quantitative analysis, ratio images (R) were generated where $R = F_{334}/F_{365}$, i.e., the fluorescence intensity at 334 nm was divided by the fluorescence intensity at 365 nm. Image processing was carried out as described previously (Linderman *et al.*, 1990).

$[Ca^{2+}]_i$ calibration

Calibration measurements were obtained by imaging three solutions in the flow chamber: for saturated calcium, a so-

lution of 10 μM fura-2 free acid (Molecular Probes) in 10 mM HEPES, 150 mM KCl, 500 μM $CaCl_2$, and 0.2% NaN_3, pH 7.4; for low calcium, 10 μM fura-2 free acid in the above KCl/HEPES solution with 5 mM ethylene glycol-bis(β-aminoethyl ether)-*N,N,N′,N′*-tetraacetic acid (EGTA) replacing $CaCl_2$; and for background subtraction, the KCl/HEPES solution with EGTA and no fura-2 free acid. Intracellular-free $[Ca^{2+}]$ was determined according to the equation $[Ca^{2+}]_i = K_d\beta(R - R_{min})/(R_{max} - R)$, where K_d = 224 nM is the equilibrium dissociation constant for fura-2 and Ca^{2+} (Grynkiewicz *et al.*, 1985), $\beta = F_{365}$(no calcium)/F_{365}(saturating Ca^{2+}), $R_{max} = (F_{334}/F_{365})$ at saturating $[Ca^{2+}]$, and $R_{min} = (F_{334}/F_{365})$ with $[Ca^{2+}] = 0$. Corrections for differences between KCl/HEPES viscosity and intracellular viscosity were made as previously described (Linderman *et al.*, 1990).

Analysis of single cells was accomplished by a region-of-interest masking technique that determined the spatially averaged value of the fluorescence intensity or calcium concentration for each cell as a function of time. A one bit overlay mask of the cell corresponding to portions of the image with fluorescence intensity above a user-set threshold level was created. The average of all pixel data that fell under the mask was computed, excluding pixels for which the denominator value was zero.

Acknowledgments

We thank Nick Layzer for his assistance with the ELISA EGF assay. We also thank Jennifer Linderman and Linda Slakey for helpful discussions. This work was supported by the National Science Foundation under grant DMB-8803826.

Received: March 14, 1991.
Revised and accepted: July 24, 1991.

References

Bellot, F., Moolenaar, W., Kris, R., Mirakhur, B., Verlaan, I., Ullrich, A., Schlessinger, J., and Felder, S. (1990). High-affinity epidermal growth factor binding is specifically reduced by a monoclonal antibody, and appears necessary for early responses. J. Cell. Biol. *110,* 491–502.

Berridge, M.J., and Irvine, R.F. (1984). Inositol trisphosphate: a novel second messenger in cellular signal transduction. Nature (Lond.) *312,* 315–321.

Bjorge, J.D., Chan, T.-O., Antczak, M., Kung, H.-J., and Fujita, D.J. (1990). Activated type I phosphatidylinositol kinase is associated with the epidermal growth factor (EGF) receptor following EGF stimulation. Proc. Natl. Acad. Sci. USA *87,* 3816–3821.

Chapron, Y., Cochet, C., Crouzy, S., Jullein, T., Kiramidas, M., and Verdetti, J. (1989). Tyrosine protein kinase activity of the EGF receptor is required to induce activation of receptor-operated calcium channels. Biochem. Biophys. Res. Commun. *158,* 527–533.

Chen, W.S., Lazar, C.S., Poenie, M., Tsien, R.Y., Gill, G.N., and Rosenfeld, M.G. (1987). Requirement for intrinsic protein tyrosine kinase in the immediate and late actions of the EGF receptor. Nature (Lond.) *328,* 820–823.

Chock, P.B., Rhee, S.G., and Stadtman, E.R. (1980). Interconvertible enzyme cascades in cellular regulation. Annu. Rev. Biochem. *49,* 813–843.

Cochet, C., Gill, G.N., Meisenhelder, J., Cooper, J.A., and Hunter, T. (1984). C-kinase phophorylates the epidermal growth factor receptor and reduces its epidermal growth factor-stimulated tyrosine protein kinase activity. J. Biol. Chem. *259,* 2553–2558.

Defize, L.K.H., Arndt-Jovin, D.J., Jovin, T.M., Boonstra, J., Meisenhelder, J., Hunter, T., de Hey, H.T., and de Laat, S.W. (1988). A431 cell variants lacking the blood group A antigen display increased high affinity epidermal growth factor-receptor number, protein-tyrosine kinase activity, and receptor turnover. J. Cell Biol. *107,* 939–949.

Defize, L.K.H., Boonstra, J., Meisenhelder, J., Kruijer, W., Tertoolen, L.G.J., Tilly, B.C., Hunter, T., van Bergen en Henegouwen, P.M.P., Moolenaar, W.H., and de Laat, S.W. (1989). Signal transduction by epidermal growth factor occurs through the subclass of high affinity receptors. J. Cell Biol. *109,* 2495–2507.

Downward, J., Parker, P., and Waterfield, M.D. (1984). Autophosphorylation site on the epidermal growth factor receptor. Nature (Lond.) *311,* 483–485.

Dupont, G., Berridge, M.J., and Goldbeter, A. (1990). Latency correlates with period in a model for signal-induced Ca^{2+} oscillations based on Ca^{2+}-induced Ca^{2+} release. Cell Regul. *1,* 853–861.

Fearn, J.C., and King, C.A. (1985). EGF receptor affinity is regulated by intracellular calcium and protein kinase C. Cell *40,* 991–1000.

Gonzalez, F.A., Gross, D.J., Heppel, L.A., and Webb, W.W. (1988). Studies on the increase in cytosolic free calcium induced by epidermal growth factor, serum and nucleotides in individual A431 cells. J. Cell. Physiol. *135,* 269–276.

Grynkiewicz, G., Poenie, M., and Tsien, R.Y. (1985). A new generation of Ca^{2+} indicators with greatly improved fluorescence properties. J. Biol. Chem. *260,* 3440–3450.

Hepler, J.R., Norimichi, N., Lovenberg, T.W., DiGuiseppi, J., Herman, B., Earp, S.H., and Harden, K.T. (1987). Epidermal growth factor stimulates the rapid accumulation of inositol (1,4,5)-trisphosphate and a rise in cytosolic calcium mobilized from intracellular stores in A431 cells. J. Biol. Chem. *262,* 2951–2956.

Hunter, T., Ling, N., and Cooper, A. (1984). Protein kinase C phosphorylation of the EGF receptor at a threonine residue close to the cytoplasmic face of the plasma membrane. Nature (Lond.) *311,* 480–483.

Jacob, R., Merritt, J.E., Hallam, T.J., and Rink, T.J. (1988). Repetitive spikes in cytoplasmic calcium evoked by histamine in human endothelial cells. Nature (Lond.) *335,* 40–45.

Kawamoto, T., Sato, J.D., Le, A., Polikoff, J., Sato, G.H., and Mendelsohn, J. (1983). Growth stimulation of A431 cells by epidermal growth factor: identification of high-affinity receptors for epidermal growth factor by an anti-receptor monoclonal antibody. Proc. Natl. Acad. Sci. USA *80,* 1337–1341.

Kim, J.W., Sim, S.S., Kim, U.-H., Nishibe, S., Wahl, M.I., Carpenter, G., and Rhee, S.G. (1990). Tyrosine residues in bovine phospholipase C-γ phosphorylated by the epidermal growth factor receptor *in vitro.* J. Biol. Chem. *265,* 3940–3943.

Kuppaswamy, D., and Pike, L.J. (1989). Ligand-induced desensitization of ^{125}I-epidermal growth factor internalization. J. Biol. Chem. *264,* 3357–3363.

Lax, I., Bellot, F., Honegger, A.M., Schmidt, A., Ullrich, A., Givol, D., and Schlessinger, J. (1990). Domain deletion in the extracellular portion of the EGF-receptor reduces ligand binding and impairs cell surface expression. Cell Regul. *1,* 173–188.

Linderman, J.J., Harris, L.J., Slakey, L.L., and Gross, D.J. (1990). Charge-coupled device imaging of rapid calcium transients in cultured arterial smooth muscle cells. Cell Calcium *11,* 131–144.

Margolis, B., Rhee, S.G., Felder, S., Mervic, M., Lyall, R., Levitzki, A., Ullrich, A., Zilberstein, A., and Schlessinger, J. (1989). EGF tyrosine phosphorylation of phospholipase C-II: a potential mechanism for EGF receptor signalling. Cell *57,* 1101–1107.

Marty, A., Horn, R., Tan, Y.P., and Zimmerberg, J. (1989). Delay of the Ca mobilization response to muscarinic stimulation. In: *Secretion and Its Control,* ed. G.S. Oxford and C.M. Armstrong, New York: Rockefeller Univ. Press, 97–110.

Meisenhelder, J., Suh, P.-G., Rhee, S.G., and Hunter, T. (1989). Phospholipase C-γ is a substrate for the PDGF and EGF receptor protein-tyrosine kinases in vivo and in vitro. Cell *57,* 1109–1122.

Meyer, T., Holowka, D., and Stryer, L. (1988). Highly cooperative opening of calcium channels by inositol 1,4,5-trisphosphate. Science *240,* 653–656.

Miledi, R., and Parker, I. (1989). Latencies of membrane currents evoked in *Xenopus* oocytes by receptor activation, inositol trisphosphate and calcium. J. Physiol. *415,* 189–210.

Moolenaar, W.H., Aerts, R.J., Tertoolen, L.G.J., and de Laat, S.W. (1986). The epidermal growth factor induced calcium signal in A431 cells. J. Biol. Chem. *261,* 279–284.

Moolenaar, W.H., Bierman, A.J., Tilly, B.C., Verlaan, I., Defize, L.H.K., Honegger, A.M., Ullrich, A., and Schlessinger, J. (1988). A point mutation at the ATP-binding site of the EGF-receptor abolishes signal transduction. EMBO J. *7,* 707–710.

Mozhayeva, G.N., Naumov, A.P., and Kuryshev, Y.A. (1989). Epidermal growth factor activates calcium-permeable channels in A431 cells. Biochim. Biophys. Acta *1011,* 171–175.

Nishizuka, Y. (1984). The role of protein kinase C in cell surface signal transduction and tumour promotion. Nature (Lond.) *308,* 693–698.

Pandiella, A., Malgaroli, A., Meldolesi, J., and Vicentini, L.M. (1987). EGF raises cytosolic Ca^{2+} in A431 and Swiss 3T3 cells by dual mechanism. Exp. Cell Res. *170,* 175–185.

Parker, I., and Miledi, R. (1986). Changes in intracellular calcium and membrane currents evoked by injection of inositol trisphosphate into Xenopus oocytes. Proc. R. Soc. Lond. B Biol. Sci. *228,* 307–315.

Pike, L.J., and Eakes, A.T. (1987). Epidermal growth factor stimulates the production of phosphatidylinositol monophosphate and breakdown of polyphosphoinositides in A431 cells. J. Biol. Chem. *262,* 1644–1651.

Rooney, T.A., Sass, E.J., and Thomas, A.P. (1989). Characterization of cytosolic calcium oscillations induced by phenylephrine and vasopressin in single fura-2-loaded hepatocytes. J. Biol. Chem. *264,* 17131–17141.

Sawyer, S.T., and Cohen, S. (1981). Enhancement of calcium uptake and phosphatidylinositol turnover by epidermal growth factor in A431 cells. Biochemistry *20,* 6280–6286.

Stadtman, E.R., and Chock, P.B. (1979). Advantages of enzyme cascades in the regulation of key metabolic processes. In: *The Neurosciences Fourth Study Program,* ed. F.O. Schmitt and F.G. Worden, Cambridge: MIT Press, 801–817.

Thompson, D.M., Cochet, C., Chambaz, E.N., and Gill, G.N. (1985). Separation and characterization of a phosphatidyl inositol kinase activity that co-purifies with the epidermal growth factor receptor. J. Biol. Chem. *260,* 8824–8830.

Todderud, G., Wahl, M.I., Rhee, S.G., and Carpenter, G. (1990). Stimulation of phospholipase C-γI membrane association by epidermal growth factor. Science *249,* 296–298.

Walker, D.H., and Pike, L.J. (1987). Phosphatidyl inositol kinase is activated in membranes derived from cells treated with epidermal growth factor. Proc. Natl. Acad. Sci. USA *84,* 7513–7517.

Wahl, M., Daniel, T.O., and Carpenter, G. (1989a). Antiphosphotyrosine recovery of phospholipase C activity after EGF treatment of A431 cells. Science *241,* 968–970.

Wahl, M.I., Nishibe, S., Kim, J.W., Kim, H., Rhee, S.G., and Carpenter, G. (1990). Identification of two epidermal growth factor-sensitive tyrosine phosphorylation sites of phospholipase C-γ in intact HSC-1 cells. J. Biol. Chem. *265,* 3944–3948.

Wahl, M.I., Nishibe, S., Suh, P.-G., Rhee, S.G., and Carpenter, G. (1989b). Epidermal growth factor stimulates tyrosine phosphorylation of phospholipase C-II independently of receptor internalization and extracellular calcium. Proc. Natl. Acad. Sci. USA *86,* 1568–1572.

Wahl, M., Sweatt, D.J., and Carpenter, G. (1987). Epidermal growth factor (EGF) stimulates inositol trisphosphate formation in cells which overexpress the EGF receptor. Biochem. Biophys. Res. Commun. *142,* 688–695.

Wiley, H.S. (1988). Anomalous binding of epidermal growth factor to A431 cells is due to the effect of high receptor densities and a saturable endocytic system. J. Cell Biol. *107,* 801–810.

Woods, N.M., Cuthbertson, K.S.R., and Cobbold, P.H. (1986). Repetitive transient rises in cytoplasmic free calcium in hormone stimulated hepatocytes. Nature (Lond.) *319,* 600–602.